Forensic Assessment of Textile Fibers Using Micro FTIR-ATR Spectroscopy

Samara Testoni *, Rafael Ortiz , Kristiane Mariotti , Flavio Camargo

Posted Date: 23 May 2023

doi: 10.20944/preprints202305.1640.v1

Keywords: forensic sciences; crime scene; trace evidence; spectroscopy; polyethylene.

Article

Forensic Assessment of Textile Fibers Using Micro FTIR-ATR Spectroscopy

Samara Testoni [1,*], Rafael Ortiz [2], Kristiane Mariotti [2], and Flavio Camargo [1]

[1] Federal University of Rio Grande do Sul 1; testonisamara@gmail.com, fcamargo@ufrgs.br
[2] Federal Police Department 2; ortiz.rs@gmail.com, krismariotti@gmail.com
* Correspondence: testonisamara@gmail.com

Abstract: Forensic assessments may involve the sampling of textile fibers when examining crime scenes. The need to characterize and identify those fibers is crucial as they can provide extensive information relating to a crime, linking a suspect to a location. Fibers in particular may contain issues in terms of both size and quantity of sample, and micro Fourier transform Infrared in attenuated total reflectance mode (micro FTIR-ATR) spectroscopy presents a non-destructive method to identify those fibers. In this study we carried out a rapid forensic assessment via micro FTIR-ATR of sixty textile fibers recovered from twenty white fabrics relying on tape lifting method, in order to discriminate those materials. Two dimensional principal component analysis and radar chart were applied to enhance the visual comparison of the fibers. Results of infrared spectra revealed that the technique allows the discrimination of textile fibers according to their spectral composition (cellulose, polyamide, polyester, or mixture of these composites) and to some characteristics, as number and width of peaks, peak position according to the wavenumber, absorbance index related to peak sharpness, etc. The technique was deemed useful in the forensic assessment of the fibers, presenting rapid and enlightening results.

Keywords: forensic sciences; crime scene; trace evidence; spectroscopy; polyethylene

1. Introduction

Microtraces are materials not visible to the naked eye, or hardly visible, which have submillimeter, submicroscopic or microscopic sizes, contributing to their ubiquity and latency in crime scenes. Due to their tiny dimensions they are abundant at crime scenes, and present large dissemination and permanence on several surfaces, even after the removal of macroscopic traces [1,2]. Considering the Locard Exchange Principle, whenever two people come together during an assault, there is common a cross transfer of fibers of victim clothing fibers to the assailant clothing and vice. Therefore, fibers are considered trace evidence and have distinctive qualitative (morphological characteristics such as color, opacity, brilliance, thickness, diameter, roughness) and quantitative (content of chemical composites as polyester, C-O bonds, percentage of absorbance and transmittance, among others) characteristics [3–5]. Besides fibers, other types of trace evidence include glass shards, hair, soils and paints etc.

Widely known as trace evidence, fibers are minute portions of several materials which are manufactured in large amounts and distributed throughout the world to compose textile subproducts we use in our everyday lives, such as clothing [6,7]. Fabrics are made from several fibers formed into tiny and thin yarns used to compose the textile, and given the variety typed of fabrics, it is common to find many distinct fibers, produced in numerous different ways, with different colors and several compositions (natural and manmade fibers). Once recovered from a crime scene and compared in the laboratory, a variety of analytical techniques may help to identify, characterize and assess the composition of the fibers. Nevertheless, the value of the fiber evidence and any other material found in a crime scene depends on the early circumstances, particularly of the case and on the factors at the moment of the sampling, because these steps are fundamental to investigate that

 doi:10.20944/preprints202305.1640.v1

the fiber share a common origin. Although the common source is not certain once there are thousands of fibers made the same, it is crucial to exclude several possibilities of origin [5,8].

As each of the distinct types of fibers present unique chemical compositions, the infrared microscopy may assist with the identification of manmade fibers, such as acrylic which is made from polyacrylonitrile, polyester from polyethylene terephthalate, nylon from polyamide, and rayon from cellulose [9–11]. Despite the wide classes of fibers, peculiarities may be identified in their chemical profile due to variations in specific composites; as example, it is possible to find identify types of acrylic fibers with different mixtures of co-polymers by infrared spectroscopy [2,6,7]. When deciding the analytical methods to use it is fundamental to consider the destructive nature as well as discriminatory power of a technique. Spectroscopic techniques have shown to be appropriate for the assessment of fibers, being particularly important to screen different samples including textile materials [12–14]. Infrared spectroscopy is a valuable technique of fibers comparison and identification in forensic analyses, as previously shown in other works [2,9,15,16].

To simplify the IR analysis of individual fibers and making the method practicable for routine use in the forensic laboratories is recommended to couple the IR microscope with Fourier transform infrared (FTIR) spectrometers. Microscopy is a combination of spectrometers with optical microscopic system which allows visualization and chemical investigation of a minor portion of the sample, relying on spectroscopic analysis in a microscopic scale [17–19]. By considering specific regions, the technique substantially improves the identification of trace evidence in the samples, and therefore acquires crucial relevance in forensic caseworks. Nonetheless, this technique has been widely applied in criminal investigation, mainly in studies with documentoscopy, residues of drugs and explosives in fingerprints, counterfeit medicine, natural and manmade textile fibers, among others [1,20,21]. Operationally, infrared microscopy requires an infrared source to probe absorptions in the mid-IR region of the spectrum. The radiation passes through a highly specific region of the sample (as small as 5x5 μm) by the use of distinct apertures [22]. The infrared radiation interacts with the sample allowing identification and characterization of the bonds and of the substances or mixtures present. One of the main advantages of the infrared microscope is that the material can be analyzed at high magnification with visible light, and the stage can be moved along distinct axes enabling the material to be brought into the field of view and into sharp focus prior to analysis, offering good sensitivity from the equipment [9,23].

Micro-Fourier transform infrared spectroscopy in attenuated total reflectance (ATR) is a prominent technique, which combines infrared spectroscopy with an optical microscopy approach. Also, it is a non-destructive and reproducible analysis with forensic potential to be effective in fibers characterization. In Brazil, there are no published researches with textile fibers and micro-FTIR-ATR analysis, being necessary this type of work to demonstrate the potential of this technique in the evaluation of textile fibers. In this way, the objective of this study was to explore the rapid assessment of sixty textile fibers recovered from twenty white fabrics by using micro-FTIR-ATR to discriminate them under a forensic approach. The potential of the technique will be observed with statistical analyses, relying both on the differentiation of fibers according to the spectra obtained by micro FTIR, as well as their thickness, obtained by the ATR microscope.

2. Materials and Methods

The experimental design was based on sampling 3 (three) fibers recovered via adhesive tape lifting in different locations of twenty white fabrics (3 repetitions of 20 fabrics) (Table 1, Figure 1). Of the twenty fabric samples described in Table 1, seven are made of 100% cotton (F-1, F-2, F-6, F-9, F-10, F-14 and F-20); eight fabrics are made of cotton and polyester blended (F-3, F-4, F-5, F-11, F-15, F-16, F-17 and F-18); three fabrics are composed by cotton and polyamide blended (F-7, F-8, and F-12); and only two fabrics are composed of 100% polyester (F-13 and F-19), according to the information provided by the manufacturer (tag of each fabric).

Preprints (www.preprints.org) | NOT PEER-REVIEWED | Posted: 23 May 2023 doi:10.20944/preprints202305.1640.v1

Table 1. Description of the composition of fabrics according to the manufacture.

Fabric	Fiber	Colour	Fabric type	Manufacture composition
F-1	1.1	white	face towel	100% cotton
	1.2	white	face towel	100% cotton
	1.3	white	face towel	100% cotton
F-2	2.1	white	bath towel	100% cotton
	2.2	white	bath towel	100% cotton
	2.3	white	bath towel	100% cotton
F-3	3.1	white	bed sheet	50% cotton, 50% polyester
	3.2	white	bed sheet	50% cotton, 50% polyester
	3.3	white	bed sheet	50% cotton, 50% polyester
F-4	4.1	white	cleaning cloth	95% cotton, 5% polyester
	4.2	white	cleaning cloth	95% cotton, 5% polyester
	4.3	white	cleaning cloth	95% cotton, 5% polyester
F-5	5.1	white	cleaning cloth	95% cotton, 5% polyester
	5.2	white	cleaning cloth	95% cotton, 5% polyester
	5.3	white	cleaning cloth	95% cotton, 5% polyester
F-6	6.1	white	face towel	100 % cotton
	6.2	white	face towel	100 % cotton
	6.3	white	face towel	100 % cotton
F-7	7.1	white	cleaning cloth	100% polyester
	7.2	white	cleaning cloth	100% polyester
	7.3	white	cleaning cloth	100% polyester
F-8	8.1	white	pants	100% polyester
	8.2	white	pants	100% polyester
	8.3	white	pants	100% polyester
F-9	9.1	white	pants	100 % cotton
	9.2	white	pants	100 % cotton
	9.3	white	pants	100 % cotton
F-10	10.1	white	shorts	100 % cotton
	10.2	white	shorts	100 % cotton
	10.3	white	shorts	100 % cotton
F-11	11.1	white	cleaning cloth	95% cotton, 5% polyester
	11.2	white	cleaning cloth	95% cotton, 5% polyester
	11.3	white	cleaning cloth	95% cotton, 5% polyester
F-12	12.1	white	pants	100% polyester
	12.2	white	pants	100% polyester
	12.3	white	pants	100% polyester
F-13	13.1	white	lab coat	90% cotton, 10% polyamide
	13.2	white	lab coat	90% cotton, 10% polyamide

 doi:10.20944/preprints202305.1640.v1

	13.3	white	lab coat	90% cotton, 10% polyamide
F-14	14.1	white	bed sheet	100% cotton
	14.2	white	bed sheet	100% cotton
	14.3	white	bed sheet	100% cotton
F-15	15.1	white	pillow case	50% cotton, 50% polyester
	15.2	white	pillow case	50% cotton, 50% polyester
	15.3	white	pillow case	50% cotton, 50% polyester
F-16	16.1	white	pillow case	88% cotton, 12% flax
	16.2	white	pillow case	88% cotton, 12% flax
	16.3	white	pillow case	88% cotton, 12% flax
F-17	17.1	white	cloth napkin	95% cotton, 5% polyester
	17.2	white	cloth napkin	95% cotton, 5% polyester
	17.3	white	cloth napkin	95% cotton, 5% polyester
F-18	18.1	white	cloth napkin	95% cotton, 5% polyester
	18.2	white	cloth napkin	95% cotton, 5% polyester
	18.3	white	cloth napkin	95% cotton, 5% polyester
F-19	19.1	white	shirt	90% cotton, 10% polyamide
	19.2	white	shirt	90% cotton, 10% polyamide
	19.3	white	shirt	90% cotton, 10% polyamide
F-20	20.1	white	shirt	100% cotton
	20.2	white	shirt	100% cotton
	20.3	white	shirt	100% cotton

Preprints (www.preprints.org) | NOT PEER-REVIEWED | Posted: 23 May 2023 doi:10.20944/preprints202305.1640.v1

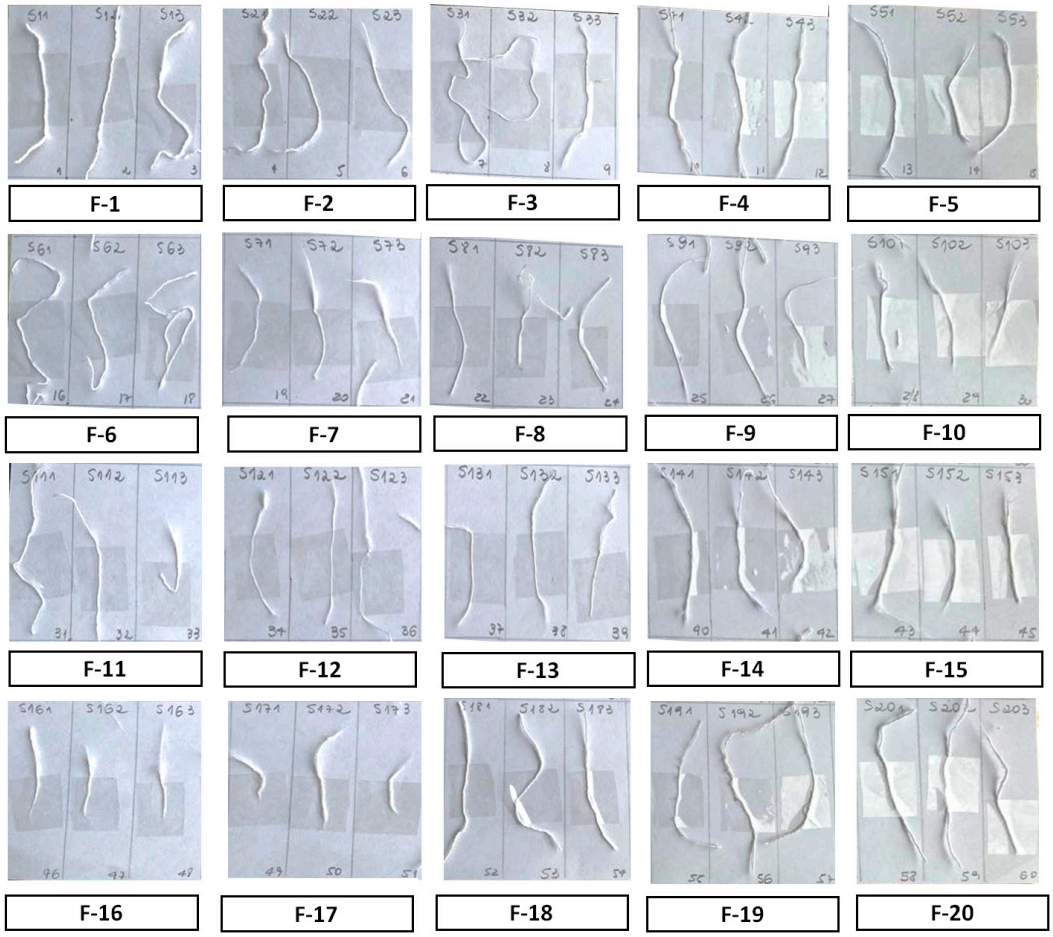

Figure 1. Images of sixty textile fibers removed from twenty white fabrics (F-1 to F-20) sampled with the tape lifting method. Description of the fibers can be seen in Table 1.

The infrared spectra were acquired through the FTIR LUMOS Microscope (Bruker Optics, Germany), operating in attenuated total reflectance mode, equipped with a germanium crystal micro ATR, motorized sample platform, mercury cadmium tellurium (MCT) detector cooled by nitrogen and silicon carbide global source. ATR mode was chosen since it is a non-destructive approach and does not require any sample preparation, even with thick fibers.

A visual inspection was performed for each sample and a microscopic image of the fiber was collected with 10% of brightness (Figure 2). From this image, a region of interest was registered for analysis by creating a matrix of 3 x 3 collection points. Using the motorized sampling platform of the equipment, each predefined position of the infrared spectrum was measured and recorded, and then associated with its spatial information, until all 9 points of the matrix were analyzed. Spectra were obtained with 32 scans, in the range of 4500 to 500 cm^{-1}, resolution of 4 cm^{-1} and aperture of 100 x 100 μm. Before acquiring the spectra of the sixty fiber samples, the ATR accessory was positioned in the air and the background spectrum was acquired. Subsequently, a simple search (individual components) and analysis of mixtures (two or more components) were performed relying on the reference of corresponding spectra resent in the software library database.

Preprints (www.preprints.org) | NOT PEER-REVIEWED | Posted: 23 May 2023 doi:10.20944/preprints202305.1640.v1

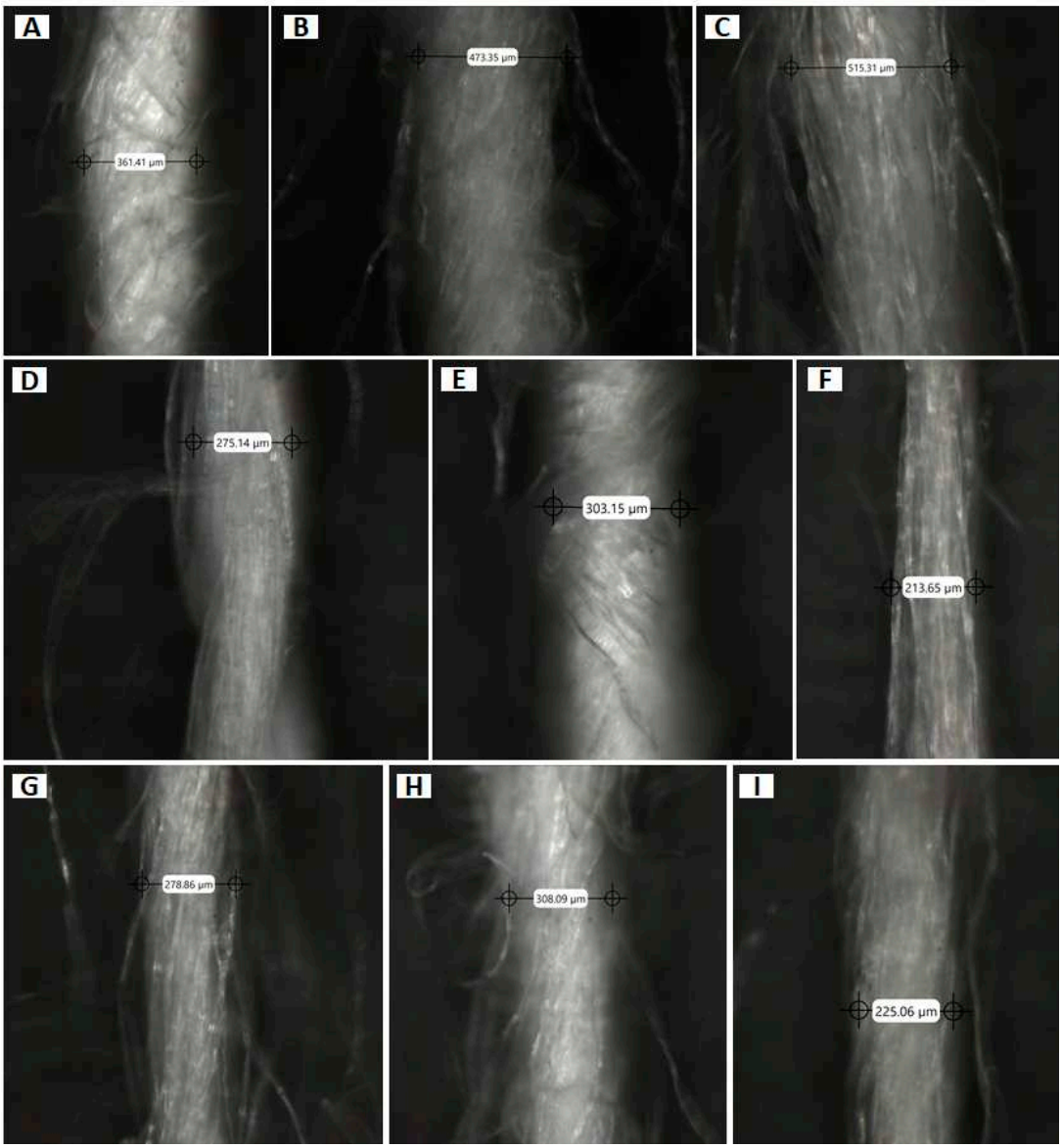

Figure 2. Images of textile fibers obtained by micro Fourier transform infrared-attenuated total reflectance (micro-FTIR -ATR) spectroscopy: 2a) F-3; 2b) F-5; 2c) F-7; 2d) F-8; 2e) F-9; 2f) F-12; 2g) F-13; 2h) F-14; 2i) F-19, with their respective diameters (µm).

Figure 3 (a, b) shows examples of infrared spectra of typical polyamide, PET and cellulose structure samples. The amount of cellulose structure in the fibers is demonstrated by the common characteristic peaks as broad peaks centered at 3300 cm^{-1} (Figure 3a), originated from the O-H bonds [25,27]. The spectral features observed to cellulose structure were relatively similar across all of the fabric fibers analyzed, and is characteristic of cotton fibers and mixtures of this composition. The sharper peak in Figure 3a at roughly 1703 cm^{-1} is indicative of polyamide (N-C, N-H and C=O bonds) and the overall configuration of neared peaks reveals the type of fiber to be acrylamide [6]. Figure 3b presents a contrasting spectrum of sample 19, in which the most relevant peak in intensity and uniqueness is around 1042 cm^{-1}, a typical position of functional groups of aromatic polyesters, such as PET - polyethylene terephthalate [9–11].

Preprints (www.preprints.org) | NOT PEER-REVIEWED | Posted: 23 May 2023 doi:10.20944/preprints202305.1640.v1

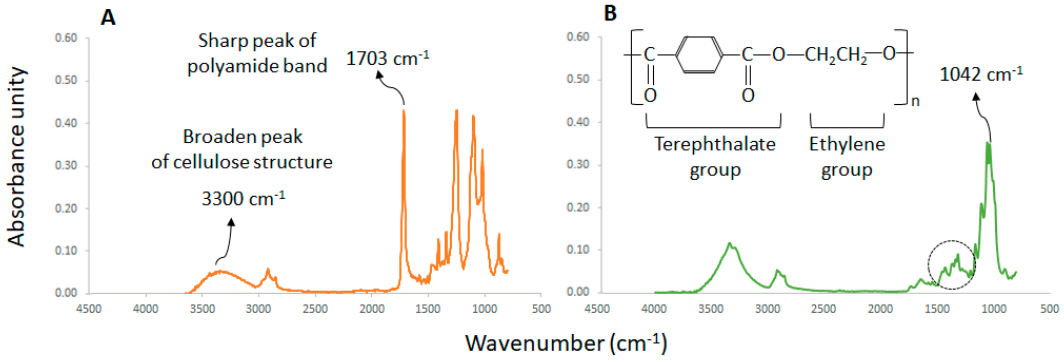

Figure 3. Micro-Fourier transform infrared-attenuated total reflectance (micro-FTIR-ATR) spectroscopy of F-7 (3a) and F-19 (3b), according to the infrared range between 4500 and 500 cm^{-1}. Figure 3a indicates two bands at 1703 cm^{-1} and 3300 cm^{-1} (typical of polyamide and cellulose structure, respectively). Specific band for polyethylene terephthalate (1042 cm^{-1}) and their functional groups are shown in Figure 3b.

Proceeding to statistical treatment of the results, all data of the spectra was compiled in a single table. Values of the absorbance and wavenumber data was taken for the triplicates of each fabric, accounting 60 samples. Two-dimensional principal component analysis (PCA) was carried out to verify the grouping of samples according to their characteristics of similarity and discrimination, and to compare these clusters with the spectra obtained by micro-FTIR-ATR analysis. Additionally, it was performed a radar chart, which is a graphical method of displaying multivariate data in the form of a two-dimensional chart of three or more quantitative variables represented on axes starting from the same point. The relative position and angle can be applied to sort the variables (axes) into relative positions that reveal distinct correlations and other comparative measures. Both PCA and radar chart analyzes were carried out in Paleontological Statistics software (PAST) [24].

3. Results and Discussion

Every feature of the spectrum may reveal inter-sample variability and the infrared absorption spectrum of molecular composites contains peaks that can be related to functional groups and may distinguish samples according to their spectrum, being fundamental in forensic analysis. The average spectra of each fiber belonging to the twenty fabrics showed differences between the observed bands and the spectral composition identified for each fiber via micro-FTIR. To proceed with the average of the spectra, data of the sixty fibers collected related to absorbance index (between 4500 and 500 cm^{-1}) were compiled in a table (Supplemental material S1). Subsequently, averaged data of triplicated fibers for each fabric was compiled in a new spreadsheet, and the discussion and presentation of the spectra in this work was relying on these twenty averages obtained (Supplemental material S2). Main differences of spectra remained in characteristics such as absorbance index (ranging from 0.1 to 0.6 a.u.), peak width (broad peaks can be associated with typical composites of cellulose structure, related to the cotton composition of the fabrics). In addition, the position of the peaks according to the absorbance index also allowed to identify composites of each sample, making it possible to discriminate them. In summary, the graphic signals shown in the IR spectra come from organic chemical bonds, and the shifts to different wavelengths come from the chemical environment that bond has around it.

Four types of chemical composition were identified by micro FTIR-ATR. Relying on the data set, a total of seven out of the initial twenty fabrics were identified as cellulose fiber (CF) type only. Eleven were a blend of cellulose fiber and polyester, polyamide or flax fibers. Only two fabric samples were identified as 100% aromatic polyester (PET).

Preprints (www.preprints.org) | NOT PEER-REVIEWED | Posted: 23 May 2023 doi:10.20944/preprints202305.1640.v1

Differently from sample 7 (Figure 3a), the typical peak of polyamide composites, around 1700 cm^{-1}, is absent. Strong bands in the spectral region between 2800 and 3000 cm^{-1} are absent to infrared spectra of polyethylene. As can be seen on Figure 3b, the dashed ellipse shows that the absorption band at 1375 cm^{-1} is slightly more intense than the one at 1470 cm^{-1}. This latter criterion is critical in order to differentiate polyethylene and polypropylene fibers. [16] studied the dependence between the microscopic features of cross-sectional shapes and the polymer type gathered by Fourier transform infrared (FTIR) spectroscopy, and also found polypropylene fibers, as well as polyvinyl chloride and modalcrylic fibers.

Figure 4a and 4b show the overlaid spectra that share similarities with each other: Figure 4a shows spectra of fabrics F-1, F-2, F-6, F-9, F-10, F-14, F-20 that present only cotton according to the manufacturer. The literature points out that the presence of broad and low absorbance peaks around 3300 cm^{-1} are typical of the cellulose structure and are related to O-H bonds. [25] analyzed chemical composition of ligno-cellulosic biomasses obtained from bamboo species by ATR-FTIR spectroscopy and they identified cellulose by similar bands. Figure 4b shows fabric samples that contain cotton and aromatic polyester in their composition indicated by the manufacturer (fabrics F-3, F-4, F-5, F-11, F-15, F-16, F-17, F -18). This composition can be stated by the differences found in the overlaid spectra in relation to those shown in Figure 4a. The peak at 3300 cm^{-1} associated with 2927 cm^{-1} are not well resolved spectra owing to the mixing of cellulose and aromatic polyester.

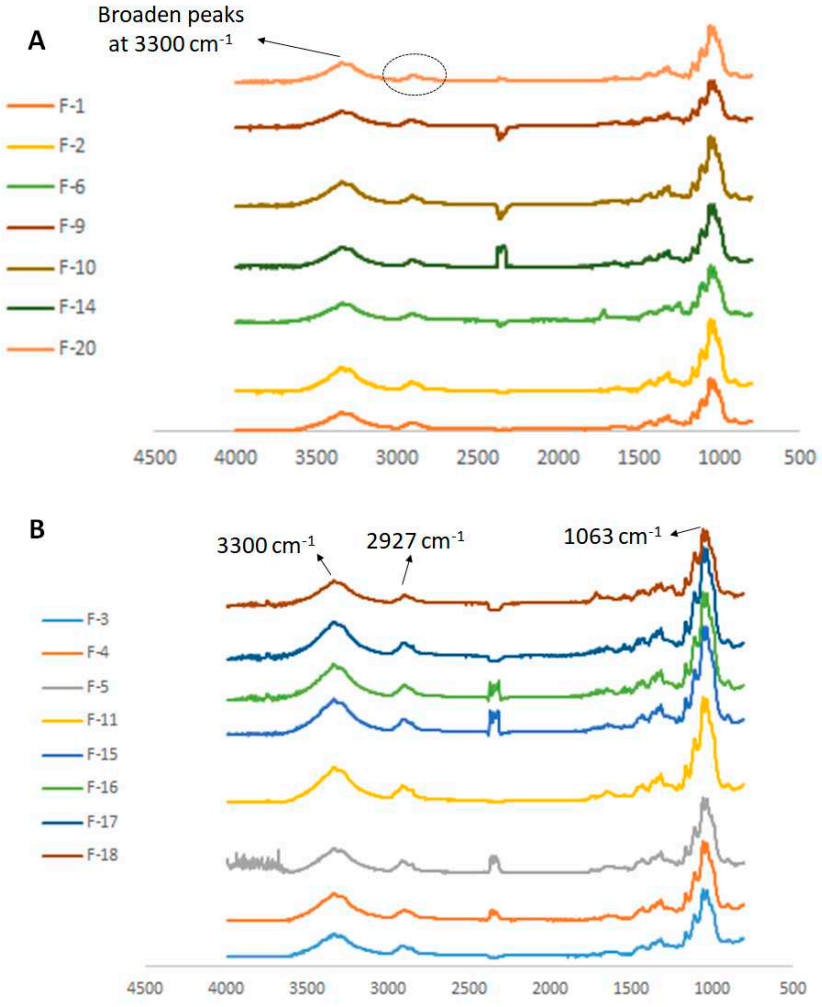

Figure 4. Overlaid spectra of pure cellulose fiber (F-1, F-2, F-6, F-9, F-10, F-14, F-20) and blended cellulose-aromatic polyester (F-3, F-4, F-5, F-11, F-15, F-16, F-17, F-18) fibers.

Furthermore, in the infrared spectrum interval between 1500 and 1000 cm^{-1}, a large number of small peaks can be observed in relation to Figure 4a. We associate these characteristics to the

Preprints (www.preprints.org) | NOT PEER-REVIEWED | Posted: 23 May 2023 doi:10.20944/preprints202305.1640.v1

composition of cellulose mixed with aromatic polyester, as previously indicated in the literature [2,7,11,25]. It was also verified the formation of slightly sharper peaks around 1063 cm^{-1} compared to the peaks of pure cellulose structure (Figure 4a). The observed distinctions regarding the spectra, both for the fabrics in 4a and 4b, can be confirmed by the composition indicated on the manufacturer tags (Table 1). This demonstrates the potential of micro-FTIR-ATR technique to be a fast and effective analysis of trace evidence such as fibers. It was also observed that F-16 was attributed to flax composition blended with cotton (Table 1). Flax produced the absorption peak at 1372 cm^{-1}, which may be assigned to C-H symmetric deformations of lignin, common to seen in flax fibers. [26] successfully used FTIR spectroscopy to investigate the effects of three treatment methods on selected physical and chemical properties of flax fibers. [27] also verified bands of flax around 1370 cm^{-1} and found dichroic bands of cellulosic fibers to distinguish flax and hemp fibers.

The overlaid spectra in Figure 5a,b were presented separately because it was distinctive features in relation to the other fabrics. Figure 5a shows a not well-resolved peak around 3300 cm^{-1} and also sharp peaks with large absorbance index around 1727 and 1108 cm^{-1}. While in figure 4b are the fabrics containing cellulose mixed with polyester, these bands are typical of pure polyester and are in agreement with the composites indicated by the manufacture (F-7, F-8 and F-12, Table 1). Only for these three fabrics occurred spectra with sharpness and larger absorbance index around 1727 cm^{-1}, as mentioned. Figure 5b shows two fabrics (F-13 and F-19) with well-resolved bands around 3300 and 2927 cm^{-1}. These peaks are typical of polyamide spectra, and are also in accordance with the manufacturer tag (Table 1). The main differences between polyester (Figure 5a) and cellulose plus polyamide mixture (Figure 5b) is the symmetry and sharpness of the peaks. As can be seen on figure 5a, fabrics with pure polyester showed a sharp peak around 1063 cm^{-1}, predominating over the near peaks located from 1500 and 1000 cm^{-1}. These features were also stated by other works, as [14] which analyzed fiber polymers using Micro-FTIR and obtained optimal matches (averagely 80%).

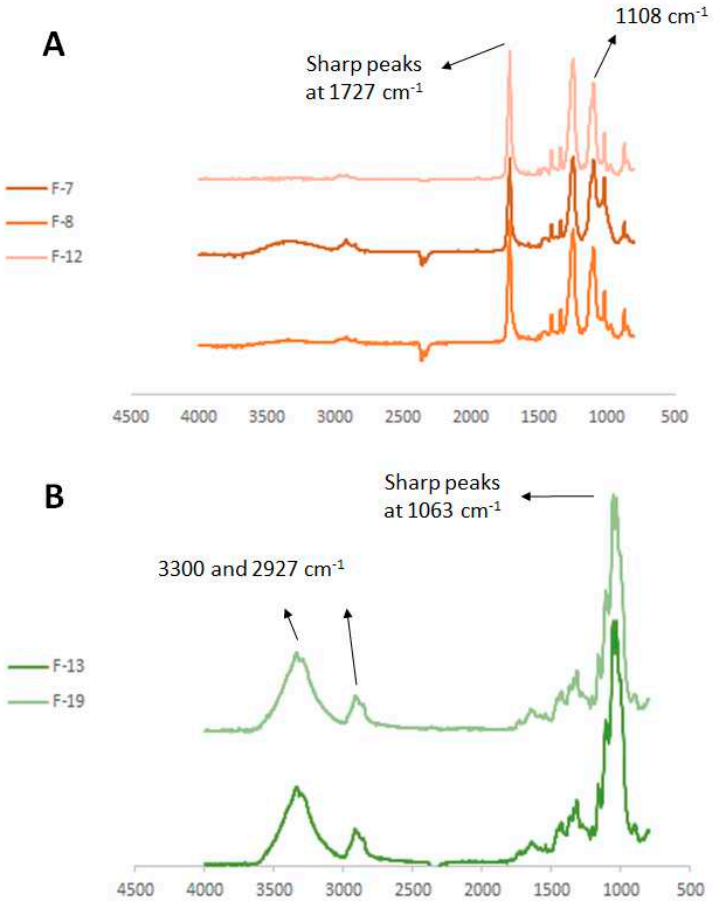

Preprints (www.preprints.org) | NOT PEER-REVIEWED | Posted: 23 May 2023 doi:10.20944/preprints202305.1640.v1

Figure 5. Overlaid spectra of pure polyester (F-7, F-8, F-12, orange) and blended polyamide-cellulose (F-13 and F-19, green) fibers.

Two dimensional PCA (principal component 1 and principal component 2) analysis showed clusterings consistent with the similarities between overlaid spectra aforementioned in Figures 4 and 5. Overall, it was verified four main clusters which revealed intra and intersimilarity among the fibers, positioned in different positive and negative principal components (quadrants). In Figure 5a, the spectra of fabrics F-7 and F-8 showed similar features and in PCA they are dispersed in the same quadrant close to each other (samples 7.1, 7.3, 8.1, 8.2 and 8.3 highlighted by the ellipse, Figure 6). Such dispersion presented positive PC1 and negative PC2 and corroborates the shared characteristics among the samples, particularly to the presence of pure polyester, as aforementioned. Other ellipses also highlight samples with homogeneous composition among themselves (Figure 6), such as samples that contain cellulose fiber as the main component (F-6, F-9, F-10 and F-15) positioned in positive PC1 and PC2. The remaining samples are positioned in negative PC1 and PC2 and represent a mixture of cellulose with aromatic polyester fibers. Likewise, samples made of polyamide and cellulose (F-13 and F-19) were disposed close to each other (negative PC1 and PC2).

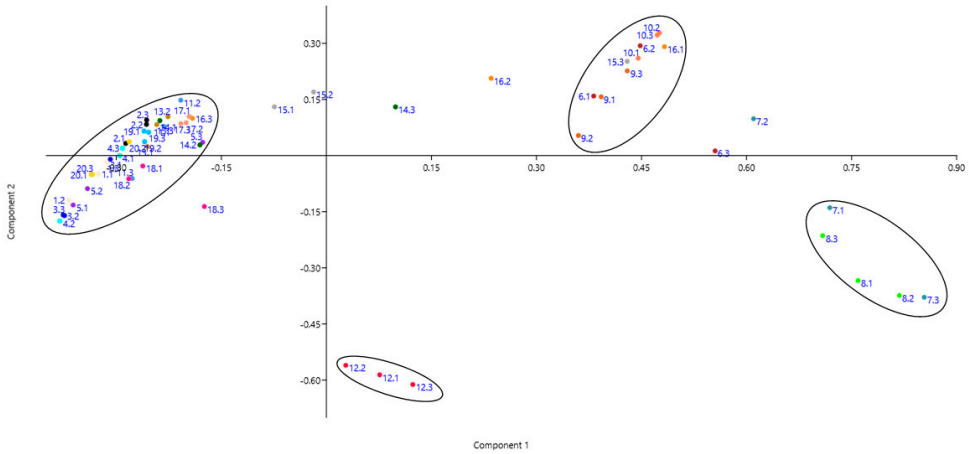

Figure 6. Two-dimensional analysis of PCA for the twenty white fabrics analyzed. The ellipses in brown, green, blue and red represent groupings according to their spectral composition.

The radar chart (Figure 7) shows the behavior of the twenty white fabrics analyzed, in which different color represents each of the fabrics. Numbers in blue are the wavenumber intervals (between 4500 and 500 cm^{-1}) and numbers in black represent the achieved absorbance indexes (0.0 to 0.6 a.u.). This graph presents a sequence of interrelated rays where each ray represents one of the obtained variables. A line is drawn connecting the data values for each ray, and highlighting outliers and commonality similarly to the PCA analysis [24]. In this way, it can be seen that samples F-7, F-8 and F-12 are outliers as they are farther from the center and clearly differ from the other samples, as similarly observed in the PCA analysis (Figure 6) and in the differentiation of the spectra presented in Figures 4 and 5. On the other hand, samples that shared similar variables were concentrated closer to the center of the radar chart, evidencing their similarities.

Preprints (www.preprints.org) | NOT PEER-REVIEWED | Posted: 23 May 2023 doi:10.20944/preprints202305.1640.v1

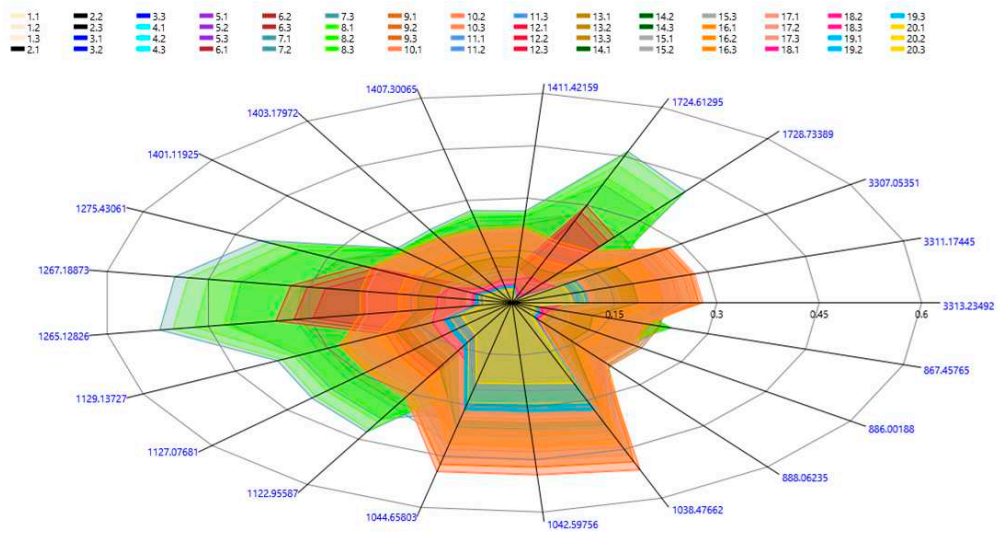

Figure 7. Radar chart for the twenty white fabrics analyzed. Colors represent each fabric, numbers in blue are the wavenumbers (cm^{-1}) and numbers in black are the absorbance indexes, respectively obtained via micro-FTIR-ATR.

4. Conclusions

Results showed that micro FTIR-ATR analysis associated to the statistical analyzes revealed potential in the discrimination of textile fibers according to their spectral composition (cellulose, polyamide, polyester, flax, or mixture of these composites). Relying on the identification of details of the spectra such as the absorbance index, sharpness and width of peaks, bands position in the wavenumber interval, and numbers of peak, it was possible to differentiate the fibers according to their provenance under a reproductively and non-destructively manner, allowing the recovery of the material for additional analyses. Therefore, micro FTIR-ATR was deemed useful for forensic assessment of fibers, revealing rapid and enlightening results.

Supplementary Materials: The following supporting information can be downloaded at the website of this paper posted on Preprints.org. Table S1: Averaged fibers; Table S2: averaged fabrics.

Author Contributions: Conceptualization, R.O. and S.T.; methodology, R.O., S.T. and K.M.; software, S.T.; validation, R.O., S.T., K.M. and F.C.; formal analysis, S.T. and K.M.; investigation, R.O., S.T. and K.M.; resources, R.O. and F.C.; data curation, S.T.; writing—original draft preparation, R.O., S.T., K.M. and F.C.; writing—review and editing, R.O., S.T., K.M. and F.C.; visualization, R.O., S.T.; supervision, R.O. and F.C.; project administration, R.O. and F.C.; funding acquisition, R.O. and F.C. All authors have read and agreed to the published version of the manuscript.

Funding: This research was funded by CNPq (grant no. 106602/2023-3) under the Project number 465450/2014-8 (INCT Forense).

Conflicts of Interest: The authors declare no conflict of interest.

References

1. Khandasammy, S.R.; Fikiet, M.A.; Mistek, E.; Ahmed, Y.; Halámková, L.; Bueno, J.; Lednev, I.K. Bloodstains, paintings, and drugs: Raman spectroscopy applications in forensic science. *Forensic Chem* **2018**, *8*, 111–133.
2. Matsushita, R.; Watanabe, S.; Iwai, T.; Nakanishi, T.; Takatsu, M.; Honda, S.; Funaki, F.; Ishikawa, T.; Seto, Y. Forensic discrimination of polyester fibers using gel permeation chromatography. *Forensic Chem* **2022**, *30*, 100428.
3. Bisbing, R.E. The forensic comparison of soil and geologic microtraces. In Forensic Chemistry: Fundamentals and Applications, First ed.; Siegel, J.A., Ed.; John Wiley & Sons, Ltd: EUA, 2016, pp. 273-317.

4. Dmitruk, W.; Brożek-Mucha, Z. 6. Forensic Analysis of Microtraces. In Inorganic Trace Analytics: Trace Element Analysis and Speciation, Matusiewicz, H., Bulska E., Eds.; De Gruyter: Berlin, Boston, 2018, pp. 276-301.
5. Gładysz, M.; Król, M.; Kościelniak, P. Current analytical methodologies used for examination of lipsticks and its traces for forensic purposes. *Microchem J* **2021**, *164*, 106002.
6. Zapata, F.; Ortega-Ojeda, F.E.; García-Ruiz, C. Forensic examination of textile fibers using Raman imaging and multivariate analysis. *Spectrochim. Acta - Part A Mol. Biomol. Spectrosc* **2022,** *268*, 120695.
7. Bianchi, F.; Riboni, N.; Trolla, V.; Furlan, G.; Avantagiatto, G.; Iacobellis, G.; Careri, M. Differentiation of aged fibers by Raman spectroscopy and multivariate data analysis. *Talanta* **2016**, *154*, 467–473.
8. Ritz, K.; Dawson, L.; Miller, D. *Criminal and Environmental Soil Forensics* **2008**.
9. Kisler-Rao, A.E. Comparison of Nylon, Polyester, and Olefin Fibers Using FTIR and Melting Point Analysis. *J. Am. Soc. Trace Evid. Exam* **2015** *6*, 1–30.
10. Miranda, K.L.; Ortega-Ojeda, F.E.; García-Ruíz, C.; Martínez, P.S. Shooting distance estimation based on gunshot residues analyzed by XRD and multivariate analysis. *Chemom. Intell. Lab. Syst.* **2019**, *193*, 103831.
11. Farrugia, K.J.; Bandey, H.; Dawson, L.; Nic Daéid, N. Chemical enhancement of soil based footwear impressions on fabric. *Forensic Sci. Int.* **2012**, *219*, 12–28.
12. Perret, E.; Sharma, K.; Tritsch, S.; Hufenus, R. Reversible mesophase in stress-annealed poly (3-hydroxybutyrate) fibers : A synchrotron x-ray and polarized ATR-FTIR study. *Polymer (Guildf)* **2021**, *231*, 124-141.
13. Yousef, S.; Eimontas, J.; Stri, N.; Subadra, S.P.; Ali, M. Thermal degradation and pyrolysis kinetic behaviour of glass fiber-reinforced thermoplastic resin by TG-FTIR, Py-GC/MS, linear and nonlinear isoconversional models. *J. Mater. Res. Technol.* **2021**, *15*, 5360-5374.
14. Corami, F.; Rosso, B.; Bravo, B.; Gambaro, A.; Barbante, C. A novel method for purification, quantitative analysis and characterization of microplastic fibers using Micro-FTIR. *Chemosphere* **2020**, *238*, 124564.
15. Coletti, F.; Romani, M.; Ceres, G.; Zammit, U.; Guidi, M. C. Evaluation of microscopy techniques and ATR-FTIR spectroscopy on textile fibers from the Vesuvian area: A pilot study on degradation processes that prevent the characterization of bast fibers. *J. Archaeol. Sci. Reports* **2021,** *36*, 102794.
16. Yogi, T.A.J.; Penrod, M.; Holt, M.; Buzzini, P. The relationship between cross-sectional shapes and FTIR profiles in synthetic wig fibers and their discriminating abilities — An evidential value perspective. *Forensic Sci. Int.* **2018,** *283*, 94–102.
17. Zięba-Palus, J.; Kunicki, M. Application of the micro-FTIR spectroscopy, Raman spectroscopy and XRF method examination of inks. *Forensic Sci. Int.* **2006,** *158*, 164–172.
18. González-Cabrera, M.; Domínguez-Vidal, A.; Ayora-Cañada, M. J. Hyperspectral FTIR imaging of olive fruit for understanding ripening processes. *Postharvest Biol. Technol.* **2018,** *145*, 74–82.
19. Dirwono, W.; Park, J.S.; Agustin-Camacho, M.R.; Kim, J.; Park, H.M.; Lee, Y.; Lee, K.B. Application of micro-attenuated total reflectance FTIR spectroscopy in the forensic study of questioned documents involving red seal inks. *Forensic Sci. Int.* **2010,** *199*, 6–8.
20. Silva, C.S.; Pimentel, M.F.; Amigo, J.M.; García-Ruiz, C.; Ortega-Ojeda, F. Chemometric approaches for document dating: Handling paper variability. *Anal. Chim. Acta*, **2018,** *1031*, 28–37.
21. Ewing, A.V.; Kazarian, S.G. Infrared spectroscopy and spectroscopic imaging in forensic science. *Analyst* **2017**, *142*, 257–272.
22. Sugita, R.; Marumo, Y. Screening of soil evidence by a combination of simple techniques: Validity of particle size distribution. *Forensic Sci. Int.* **2001,** *122*, 155–158.
23. Dégardin, K.; Guillemain, A.; Klespe, P.; Hindelang, F.; Zurbach, R.; Roggo, Y. Packaging analysis of counterfeit medicines. *Forensic Sci. Int.* **2018**, *291*, 144–157.
24. Hammer, Ø.; Harper, D.A.T. PAST. Paleontological Statistics. Version 2.07. Reference manual. *Blackwell Publ. 351* (**2006**) doi:10.1016/j.bcp.2008.05.025.
25. Biswas, S.; Rahaman, T.; Gupta, P.; Mitra, R.; Dutta, S. Biomass and Bioenergy Cellulose and lignin profiling in seven, economically important bamboo species of India by anatomical , biochemical , FTIR spectroscopy and thermogravimetric analysis. *Biomass and Bioenergy* **2022,** *158*, 106362.
26. Cao, Y.; Chan, F.; Chui, Y. H.; Xiao, H. Characterization of flax fibers modified by alkaline, enzyme, and steam-heat treatments. *BioResources* **2012,** *7*, 4109–4121.
27. Garside, P.; Wyeth, P. Identification of cellulosic fibers by FTIR spectroscopy: Differentiation of flax and hemp by polarized ATR FTIR. *Stud. Conserv.* **2006,** *51*, 205–211.

 doi:10.20944/preprints202305.1640.v1